International Journal of Nanomedicine

Dovepress
open access to scientific and medical research

Open Access Full Text Article

ORIGINAL RESEARCH

808 nm Near-Infrared Light-Excited UCNPs@mSiO$_2$-Ce6-GPC3 Nanocomposites For Photodynamic Therapy In Liver Cancer

This article was published in the following Dove Press journal:
International Journal of Nanomedicine

International Journal of Nanomedicine downloaded from https://www.dovepress.com/
For personal use only.

Jiahe Hu,[1,*] Jialan Shi,[2,3] Yingqian Gao,[1] Wei Yang,[1] Ping Liu,[1] Qinghao Liu,[1] Fei He,[4] Chunxu Wang,[2] Tao Li,[2] Rui Xie,[1] Jiuxin Zhu,[5] Piaoping Yang[4,*]

[1]Department of Digestive Internal Medicine, Harbin Medical University Cancer Hospital, Harbin 150081, People's Republic of China; [2]Department of Hematology, The First Affiliated Hospital, Harbin Medical University, Harbin 150001, People's Republic of China; [3]Department of Surgery, VA Boston Healthcare System, Brigham and Women's Hospital, Harvard Medical School, Boston, MA 12132, USA; [4]Key Laboratory of Superlight Materials and Surface Technology, Ministry of Education, College of Material Sciences and Chemical Engineering, Harbin Engineering University, Harbin 150001, People's Republic of China; [5]Department of Pharmacology (State-Province Key Laboratories of Biomedicine-Pharmaceutics of China, Key Laboratories of Cardiovascular Medicine Research, Ministry of Education), College of Pharmacy, Harbin Medical University, Harbin 150081, People's Republic of China

*These authors contributed equally to this work

Correspondence: Jiuxin Zhu
Department of Pharmacology (State-Province Key Laboratories of Biomedicine-Pharmaceutics of ChinaKey Laboratories of Cardiovascular Medicine Research, Ministry of Education), College of Pharmacy, Harbin Medical University, Harbin 150081, People's Republic of China
Tel +86 15104557900
Email zhujiuxin@hrbmu.edu.cn

Rui Xie
Department of Digestive Internal MedicineHarbin Medical University Cancer Hospital, 150 Haping Road, Nangang District, Heilongjiang, Harbin 150081, People's Republic of China
Tel +86 138450981 17
Email rxie@hrbmu.edu.cn

Background: It is important to explore effective treatment for liver cancer. Photodynamic therapy (PDT) is a novel technique to treat liver cancer, but its clinical application is obstructed by limited depth of visible light penetration into tissue. The near-infrared (NIR) photosensitizer is a potential solution to the limitations of PDT for deep tumor tissue treatment.

Purpose: We aimed to investigate 808 nm NIR light-excited UCNPs@mSiO$_2$-Ce6-GPC3 nanocomposites for PDT in liver cancer.

Methods: In our study, 808 nm NIR light-excited upconversion nanoparticles (UCNPs) were simultaneously loaded with the photosensitizer chlorin e6 (Ce6) and the antibody glypican-3 (GPC3), which is overexpressed in hepatocellular carcinoma cells. The multi-tasking UCNPs@mSiO$_2$-Ce6-GPC3 nanoparticles under 808 nm laser irradiation with enhanced depth of penetration would enable the effective targeting of PDT.

Results: We found that the UCNPs@mSiO$_2$-Ce6-GPC3 nanoparticles had good biocompatibility, low toxicity, excellent cell imaging in HepG2 cancer cells and high anti-tumor effect in vitro and in vivo.

Conclusion: We believe that the utilization of 808 nm NIR excited UCNPs@mSiO$_2$-Ce6-GPC3 nanoparticles for PDT is a safe and potential therapeutic option for liver cancer.

Keywords: liver cancer, photodynamic therapy, upconversion nanoparticles, 808 nm NIR, GPC3, targeted therapy

Introduction

Liver cancer is an invasive tumor originating from the liver. Great progress has been made in the treatment of liver cancer. However, the 5-year survival rate for liver cancer patients is only 10.1%.[1] Thus, finding innovative and effective strategies for liver cancer is important.

Photodynamic therapy (PDT) involves the interaction of nontoxic photosensitizers, oxygen and harmless light to produce reactive oxygen species that induce tumor cell death, and it is also associated with vascular shutdown and immune system activation.[2,3] Compared with traditional cancer therapies, PDT improves the quality of life of patients and has several outstanding advantages.[4] It has been reported that using a diode laser and the photosensitizer PAD-S31, PDT induces apoptosis in human liver cancer cells.[5]

The photosensitizer is the key factor in PDT. An important parameter for PDT efficacy is the tissue-penetration distance of light.[6] The commonly used porphyrin-based

© 2019 Hu et al. This work is published and licensed by Dove Medical Press Limited. The full terms of this license are available at https://www.dovepress.com/terms.php and incorporate the Creative Commons Attribution – Non Commercial (unported, v3.0) License (http://creativecommons.org/licenses/by-nc/3.0/). By accessing the work you hereby accept the Terms. Non-commercial uses of the work are permitted without any further permission from Dove Medical Press Limited, provided the work is properly attributed. For permission for commercial use of this work, please see paragraphs 4.2 and 5 of our Terms (https://www.dovepress.com/terms.php).

compounds have low light depth penetration through tissue, making PDT only suitable for superficial cancer.[7–9] Therefore, searching for new photosensitizers with a deeper penetration ability is critical for PDT.

The "optical window" of biological tissue is in the near-infrared (NIR) spectral region of 700−1100 nm.[10,11] Upconversion nanoparticles (UCNPs) absorbing photons in the NIR range can convert low-energy wavelength excitation into high-energy emission in the ultraviolet-visible region.[12–14] After NIR excitation, the UCNPs emitting visible light can overcome the limited penetration of activated light to potentially attain full PDT potential.[15,16] Developing NIR photosensitizers is a potential solution to the PDT limitations for deep tumor tissue treatment.[17]

The most common UCNPs are doped with ytterbium ions (Yb^{3+}) as sensitizers and are excited at 980 nm,[18] but at 980 nm, UCNPs have overheating problems. Light at 808 nm can overcome this overheating problem.[19] Light with a wavelength near 800 nm also passes deeper into tissues.[20,21] Ferric hydroxide-modified UCNPs were developed for 808 nm NIR-triggered synergetic tumor therapy against hypoxia tumors.[22] It was shown that g-C3N4 coated UCNPs for 808 nm NIR-triggered phototherapy and multiple imaging.[23] The combination of CuS and g-C3N4 QDs on UCNPs was used for folic acid targeted photothermal and photodynamic cancer therapy.[24] But the 808 nm NIR-excited UCNPs nanocomposites for PDT of liver cancer were not reported.

Glypican-3 (GPC3) is highly expressed in hepatocellular carcinoma tissues, but it is hardly expressed in normal tissues.[25] It is an attractive target for hepatocellular carcinoma treatment.[26] Tang et al reported that anti-GPC3 antibody and sorafenib-loaded NPs significantly inhibited HepG2 hepatocellular cancer. These anti-GPC3-targeted NPs are promising new targeted therapies for liver cancer.[27] In our study, the photosensitizer chlorin e6 (Ce6) and the anti-GPC3 were modified onto the surface of NaGdF4:Yb:Er@NaGdF4:Yb@NaNdF4:Yb (core-shell-shell UCNPs) and we obtained the UCNPs@$mSiO_2$-Ce6-GPC3 nanocomposite. We aimed to investigate UCNPs@$mSiO_2$-Ce6-GPC3-mediated PDT in liver cancer.

Materials And Methods

Reagents And Materials

All the chemicals and reagents in this study were of analytical grade without any further purification, including Gd_2O_3 (99.99%), Yb_2O_3 (99.99%), Er_2O_3 (99.99%), Nd_2O_3 (99.99%), oleic acid (OA), cetyltrimethylammonium bromide (CTAB) and sodium fluoride (NaF), and they were from China Pharmaceutical Group Chemical Reagents Co., Ltd.). N-hydroxysuccinimide (NHS), 1-octadecane (ODE), carbodiimide (EDC), dimethyl sulfoxide (DMSO) and Ce6 were obtained from Aladdin Reagent Shanghai Co., Ltd. Cyclohexane, ammonium nitrate (NH_4NO_3), sodium trifluoroacetate (CF3COONa) and ethyl orthosilicate (TEOS) were from Beijing Beihua Fine Chemicals Co., Ltd. We bought 3-aminopropyltriethoxysilane (APTES) from Tianjin Komeo Chemical Reagent Co., Ltd. Phosphate-buffered solution (PBS), 4′,6-diamidino-2-phenylindole (DAPI), rabbit anti-GPC-3 antibody were obtained from Beijing Bioss Biological Co., Ltd. Normal liver L02 cells and liver hepatocellular carcinoma HepG2 cells were purchased from the Cell Bank of Type Culture Collection of Chinese Academy of Sciences (Shanghai, China).

Synthesis NaGdF4:Yb, Er Core Nanoparticles

The synthesis method was as follows: we mixed 1 mmol of RE $(OA)_3$ (RE = 68.5% Gd + 30% Yb + 1.5% Er), 5 mmol of NaF, 15 mL of OA and 15 mL of ODE into the reactor. To remove excess water and oxygen from the system, we stirred the mixture to 110°C under vacuum condition for 40–60 mins. The temperature of the reaction was increased to 300°C and maintained for 90 mins under the condition of nitrogen. We stopped heating and cooled the product down to room temperature.

The material was cleaned by ethanol and centrifuged for precipitation. The precipitation was dissolved in cyclohexane to centrifuge for supernatant, the supernatant was cleaned by ethanol for precipitation. The precipitates (NaGdF4:Yb, Er) were dispersed in 5 mL of cyclohexane to do the further experiment.

Synthesis Of NaGdF4:Yb, Er@NaGdF4:Yb

The 1 mmol of NaGdF4:Yb, Er, 0.8 mmol of Gd $(CF_3COO)_3$, 0.2 mmol of Yb $(CF_3COO)_3$, 1 mmol of CF_3COONa, 15 mL of OA and 15 mL of ODE were mixed into the reactor. The reactant was stirred for 10 mins at room temperature, and then heated to 120°C under vacuum condition and kept for 40–60 mins to remove excess oxygen and water. When the solution was free of bubbles, the reaction temperature was raised to 310°C and stirred for 60 mins under the condition of nitrogen permeation. The obtained

NaGdF4:Yb,Er@NaGdF4:Yb core-shell NPs were dispersed in 5 mL of cyclohexane to do the further experiment.

Synthesis Of NaGdF4:Yb, Er@NaGdF4:Yb@NaNdF4:Yb

Then, 1 mmol of NaGdF4:Yb, Er@NaGdF4:Yb NPs and 0.8 mmol of Nd $(CF_3COO)_3$, 0.2 mmol of Yb $(CF_3COO)_3$, 1 mmol of CF_3COONa, 15 mL OA and 15 mL ODE were mixed; they were stirred and heated to 120°C under vacuum for 40–60 mins to remove excess oxygen and water. Then, the temperature was raised to 310°C for 60 mins under nitrogen atmosphere. The UCNPs were dispersed in 5 mL of cyclohexane for further use.

Synthesis Of UCNPs@mSiO$_2$-Ce6 NPs

A layer of mesoporous silica was coated with NPs. Firstly, 0.1 g CTAB was completely dissolved in 20 mL water, and then 2 mL of UCNPs cyclohexane solution (concentration was 5–10 mg mL^{-1}) was added to it. Stirring at 80°C for 10 mins. Then, 10 mL of the solution, 20 mL of water, 3 mL of ethanol and 150 μL of NaOH (2 mol/L) were heated to 70°C. At this point, 150 μL TEOS reaction was added for 10 mins. The product was centrifuged with ethanol for 3 times and dispersed in 50 mL of ethanol. We added 0.25 g of NH_4NO_3 and heated to 60°C reflux for 2 hrs. The product was cleaned by ethanol for 3 times, the UCNPs@mSiO$_2$ NPs were obtained.

The UCNPs@mSiO$_2$ NPs were mixed with 20 μL APTES and 5 mL H_2O to stirred for 1 hr. At the same time, 1.5 mg of Ce6, 4 mg of NHS, 6 mg EDC of and 1 mL DMSO were mixed and stirred for 30 mins. Finally, the above solution was mixed and kept away from light for 12 hrs. It was washed twice with centrifugation, we got the UCNPs@mSiO$_2$-Ce6 NPs.

Synthesis Of UCNPs@mSiO$_2$-Ce6-GPC3 Nanocomposites

The UCNPs@mSiO$_2$ NPs were mixed with 20 μL APTES and 5 mL H_2O for 1 hr. Then, 1 mg Ce6, 10 μL GPC3 antibody, 4 mg of NHS, 6 mg of EDC and 1 mL DMSO were mixed and stirred for 2 hrs so that the carboxyl group was activated. Finally, they were mixed and the mixture was stirred for 12 hrs in the dark. The product was centrifuged and UCNPs@mSiO$_2$-Ce6-CPC3 NPs were obtained.

Characterization

X-ray diffraction (XRD) was conducted with a Rigaku D/max-TTR-III diffractometer utilizing Cu-Ka radiation (λ = 0.15405 nm). Transmission electron microscopy images were captured on an FEI Tecnai G^2S-Twin with a field emission gun operating at 200 kV. A Hitachi U-3100 spectrophotometer was used to characterize the UV-visible spectra of the samples. The solution of the UCNPs@mSiO$_2$-Ce6 (1 mg/mL) was oscillated in the constant temperature water bath oscillator, and the ultraviolet absorption spectra at 650 nm was measured before and after centrifugation (2000 rpm, 5 mins) once a day to evaluate the stability of Ce6. Fourier transform infrared (FT-IR) spectroscopy spectra were got on a Perkin-Elmer 580BIR spectrophotometer utilizing the KBr pellet as the background. The fluorescence life curves of the samples were recorded and measured using the Tektronix MSO/DPO4000 oscilloscope. Upconversion emission spectra were tested on a R955 Hamamatsu photomultiplier tube, from 400 to 800 nm, the 808 nm laser diode module (K98D08M-30W, China) was used as the irradiation source. The images of confocal microscopy were recorded by a Leica TCS SP8. All the measurements were performed at room temperature.

Cellular Uptake In Vitro

UCNPs@mSiO$_2$-Ce6-GPC3 (1 mg mL^{-1}) was incubated with normal liver L02 cells and liver hepatocellular carcinoma HepG2 cells at 37°C for 0.5 hr, 1 hr and 3 hrs, respectively. The cells were washed with PBS and fixed with 2.5% glutaraldehyde for 10 mins. After rinsing, the cells were stained with 5 μg mL^{-1} of DAPI solution per well for 10 mins. We used the confocal microscope to record the imaging of cells.

In Vitro Bio-Compatibility Using MTT Assay

The normal liver L02 cells were cultured overnight in a 96-well plate. Different concentrations (7.8, 15.6, 31.3, 62.5, 125, 250 and 500 μg mL^{-1}) of UCNPs@mSiO$_2$, UCNPs@mSiO$_2$-Ce6 or UCNPs@mSiO$_2$-Ce6-GPC3 were added to the cells. After incubation for 24 hrs, 20 μL of MTT solution (5 mg mL^{-1}) was added to each well and incubated for another 4 hrs. After discarding the mixture, 150 μL of DMSO was added to dissolve the produced formazan. The plate was put on the micro-plate reader, the absorbance values were evaluated at a 490 nm wavelength.

Hemolysis Assay Of UCNPs@mSiO$_2$-Ce6-GPC3

We used the hemolysis assay to ascertain the biocompatibility of the sample. The study was approved by the Ethics Committee of Harbin Medical University Cancer Hospital. After written informed consent, the peripheral vein blood was collected using a 21-gauge needle. This healthy donor was a non-smoker and had not taken any drugs for at least 2 weeks. The human red blood cells were got by removing the serum from blood. After washing with 0.9% saline and centrifuging, the cells were diluted to 1:10 with PBS. The 0.3 mL of diluted cells suspension was mixed with 1.2 mL of deionized water as a positive control, 1.2 mL of PBS as the negative control and 1.2 mL of varying doses of material suspensions (7.8, 15.6, 31.3, 62.5, 125, 250 and 500 μg mL^{-1}). The samples were shaken and kept stable at room temperature for 2 hrs. The mixtures were centrifuged and the absorbance of the upper supernatants was detected by 541 nm UV-visible spectroscopy. The hemolysis rate was determined by the equation:

$$\text{Hemolysis}\% = [A_{sample} - A_{control(-)}]/[A_{control(+)} - A_{control(-)}],$$

A is the absorbance of the UV−visible spectrum.

In Vitro Therapeutic Effect Using MTT Assay

The HepG2 cells (8000 cells/well) were seeded in a volume of 200 μL complete RPMI1640 per well in a 96-well plate and cultured overnight. After attaching to the bottom of the wells, the cells were incubated with RPMI1640 complete medium (control or 808 nm NIR group) or gradient concentrations (7.8, 15.6, 31.3, 62.5, 125, 250 and 500 μg mL^{-1}) of UCNPs@mSiO$_2$ (UCNPs@mSiO$_2$+808 nm NIR group), Ce6 (Ce6+808 nm NIR group), UCNPs@mSiO$_2$-Ce6 (UCNPs@mSiO$_2$-Ce6+808 nm NIR group) or UCNPs@mSiO$_2$-Ce6-GPC3 (UCNPs@mSiO$_2$-Ce6-GPC3+808 nm NIR group) for 6 hrs. The 808 nm NIR irradiation was with a pump power of 2 W cm^{-2} for 148 s. After 18-hr incubation, cell activity of the HepG2 cells was tested by standard MTT assay.

In Vivo Anti-Cancer Efficacy

The in vivo animal study was approved by the Ethics Committee of Harbin Medical University Cancer Hospital. Male nude mice (4 weeks old) were obtained from Beijing Weitong Lihua. Experimental Animal Technology Co., Ltd. The experiments were performed in compliance with the criteria of the National Regulation of China for Care and Use of Laboratory Animals. The tumors were built up by subcutaneous injection of HepG2 cells into the right axilla of each mouse. After 1 week, the tumor long diameter was about 6–8 mm. The tumor-bearing mice were divided into 5 groups randomly (n = 6, each group) and treated by normal saline, 808 nm NIR, Ce6+808 nm NIR, UCNPs@mSiO$_2$-Ce6+808 nm NIR, UCNPs@mSiO$_2$-Ce6-GPC3+808 nm NIR. For each treatment group, 0.1 mL of 1.5 mg mL^{-1} Ce6, 16.35 mg mL^{-1} UCNPs@mSiO$_2$-Ce6 (1.5 mg mL^{-1} Ce6 contained) and 32.7 mg mL^{-1} UCNPs@mSiO$_2$-Ce6-GPC3 (1.5 mg mL^{-1} Ce6 contained) were injected through the tail vein. All 808 nm NIR irradiation was 2 W cm^{-2} for 148 s. The mice were treated once every 7 days, the tumor size and body weight were assessed and recorded every 2 days.

Histology Examination

The mice were sacrificed 2 weeks later. Tumors of all groups and the major organs including heart, lung, liver, spleen and kidney were separated and sliced. After dehydration using buffered formalin, ethanol of different concentrations and xylene, the dehydrated tissues were embedded, sliced for hematoxylin and eosin staining and analyzed for pathology.

Results

Schematic Drawing And Physicochemical Characterization Of Upconversion Nanocarriers

Figure 1A shows the structure of NaGdF4:Yb:Er@NaGdF4:Yb@NaNdF4:Yb (UCNPs). We tested the XRD peak of the UCNPs and the UCNPs@mSiO$_2$ (Figure 1B). The diffraction peaks of our synthesized core-shell-shell structure UCNPs were almost completely corresponding to the standard card of hexagonal phase NaGdF4 (JCPDS No.27-0699), indicating that the nanometer particles were also the hexagonal phase structures. After the NPs were coated with a layer of mesoporous silica, we obtained the UCNPs@mSiO$_2$, it had the original diffraction peaks of the standard card, a broad peak appears at 2θ=22.0° was corresponded to the amorphous SiO$_2$. Therefore, the hexagonal phase of the UCNPs was confirmed by XRD analysis.

We used the transmission electron microscope to observe the morphology and size of the samples at different experimental stages. The NaGdF4:Yb, Er NPs had very uniform size and good dispersity in cyclohexane, the particle size was

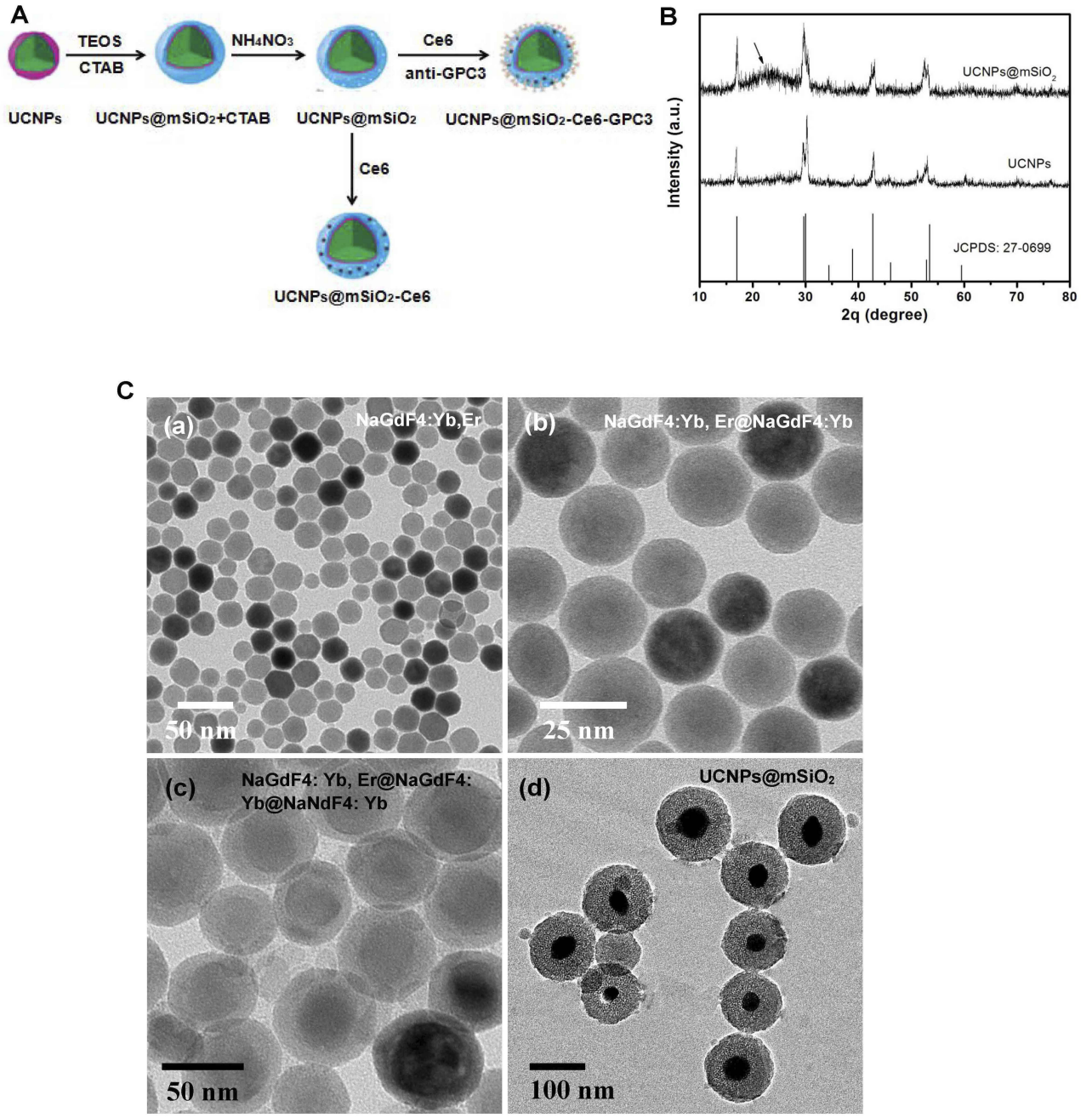

Figure 1 Characterization of UCNPs and UCNPs@mSiO$_2$. (**A**) Schematic drawing showing the fabrication process of UCNPs@mSiO$_2$-Ce6-GPC3. (**B**) XRD patterns of UCNPs, UCNPs@mSiO$_2$ and the standard XRD pattern of NaGdF4 (JCPDS No.27–0699). Representative transmission electron microscope images of (**C,** a) NaGdF$_4$:Yb, Er, (**C**, b) NaGdF$_4$:Yb, Er@NaGdF$_4$:Yb, (**C**, c) NaGdF4:Yb, Er@NaGdF4:Yb@NaNdF4:Yb (UCNPs) and (**C,** d) NaGdF4:Yb, Er@NaGdF4:Yb@NaNdF4:Yb @mSiO$_2$ (UCNPs@mSiO$_2$).

about 20 nm (Figure 1C(a)). In Figure 1C(b), we found that the chemical composition and crystal phase of NaGdF4:Yb shell and NaGdF4:Yb, Er was similar, so it was difficult to see the boundary between the NaGdF4:Yb shell and NaGdF4:Yb. The particle size of the NaGdF4:Yb, Er@NaGdF4:Yb NPs was 20–30 nm. In Figure 1C(c), the final synthesized NaGdF4:Yb, Er@NaGdF4:Yb@NaNdF4:Yb core-shell-shell structure was 30–50 nm in size. The last wrapped NaNdF4:Yb shell with a thickness between 3 and 10 nm could be clearly seen. Figure 1C(d) showed that the NaGdF4:Yb, Er@NaGdF4:Yb@NaNdF4:Yb@mSiO$_2$ (UCNPs@mSiO$_2$) was a relatively dispersed nanoparticle

with a diameter between 70 and 90 nm. In conclusion, the NPs prepared in every step had good dispersity and very uniform size in cyclohexane; the dispersity of UCNPs was kept well after SiO_2 loading.

In order to judge the photosensitizer Ce6 effect on the UV-visible absorption of the nanoparticle sample, the UV-visible absorption test was performed on the Ce6, UCNPs@$mSiO_2$ and UCNPs@$mSiO_2$-Ce6 (Figure 2A). We found that the UCNPs@$mSiO_2$ had no obvious absorption peak in the range of 350–800 nm. However, UCNPs@$mSiO_2$-Ce6 appeared obvious absorption peaks at 410 nm, 500 nm and 670 nm; this result indicated that Ce6 was absorbed near the wavelength of 410 nm, 500 nm and 670 nm. The absorbance of the solution before centrifugation was about 0.81, but the absorbance of the supernatant after centrifugation was only about 0.03 (Figure 2B). This result indicated that Ce6 was firmly loaded on UCNPs@mSiO2.

In this study, 808 nm laser was used as excitation light. To determine the effect of Ce6 on the luminescence of the NPs, the luminescence spectra of UCNPs@$mSiO_2$ and UCNPs@$mSiO_2$-Ce6 were evaluated under 808 nm NIR excitation (Figure 2C). The intensity of UCNPs@$mSiO_2$-Ce6 emitted by 808 nm NIR was lower than that of UCNPs@$mSiO_2$ under the same conditions. In particular, there was a significant reduction near the 650 nm wavelength. It overlapped with the absorption peak of Ce6 at the same wavelength. This phenomenon would likely result in resonance energy transfer from UCNPs to Ce6, which may generate singlet oxygen for PDT.

In Figure 2D, the lifetime of the two NPs decreased from 0.4953 to 0.2766 ms. It was because Ce6

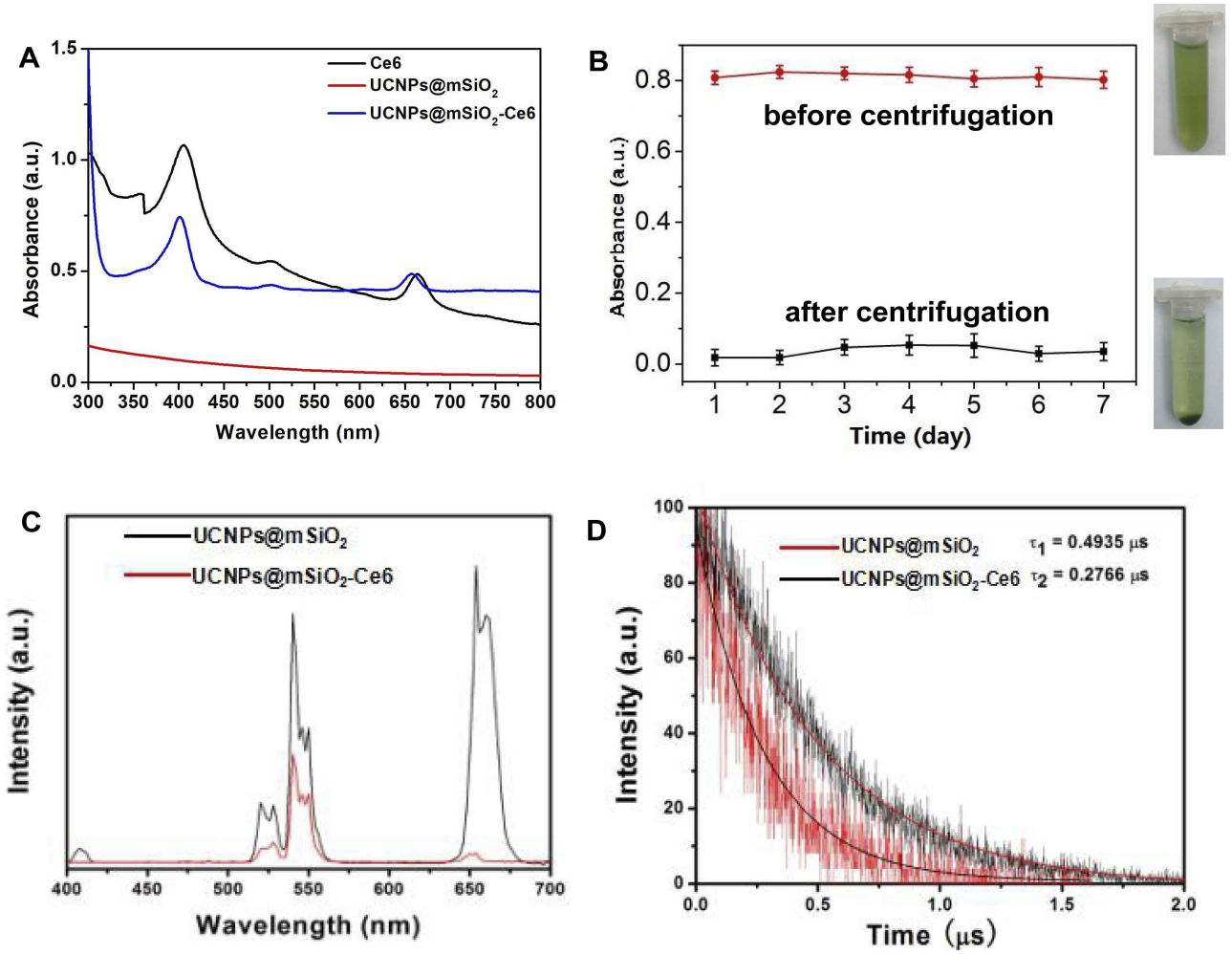

Figure 2 (**A**) UV–vis absorbance spectra of Ce6, UCNPs@$mSiO_2$ and UCNPs@$mSiO_2$-Ce6. (**B**) The ultraviolet absorption spectra at 650 nm of the UCNPs@$mSiO_2$-Ce6 (1 mg/mL) before and after centrifugation (2000 rpm, 5 mins) once a day to evaluate the stability of Ce6. (**C**) Upconversion luminescence spectra of UCNPs@$mSiO_2$ and UCNPs@$mSiO_2$-Ce6 under 808 nm excitation recorded at the same UCNPs concentration. (**D**) Decay curves of UCNPs@$mSiO_2$ and UCNPs@$mSiO_2$-Ce6 at the wavelength of 650 nm under 808 nm excitation.

absorbed some of the energy of 650 nm wavelength light generated by UCNPs@$mSiO_2$ under 808 nm laser excitation, further proving the resonance energy transfer process.

The FT-IR spectroscopy was utilized to identify the surface functional groups and apply additional evidence for successful modification. The FT-IR spectra of UCNPs@$mSiO_2$, UCNPs@$mSiO_2$-Ce6 and UCNPs@$mSiO_2$-Ce6-GPC3 were presented in Figure 3A. The band appearance located at ≈1712 cm^{-1} attributed to C=O groups indicates that the carboxyl groups of Ce6 and GPC3 antibody were successfully attached to UCNPs. Meanwhile, the peaks presented at ≈2862 cm^{-1} and ≈2953 cm^{-1} belonged to C-Hx bonds; it suggested the successful grafting of Ce6 and GPC3 antibody. In addition, the Zeta potential of UCNPs@$mSiO_2$ changed from −13 to 20.2 mV owing to the Ce6 modification (Figure 3B). After connecting GPC3 antibody, the potential dropped to 8.94 mV. The Ce6-loading efficiency of UCNPs@$mSiO_2$ examined using UV-visible spectroscopy was calculated to be≈93.34%.

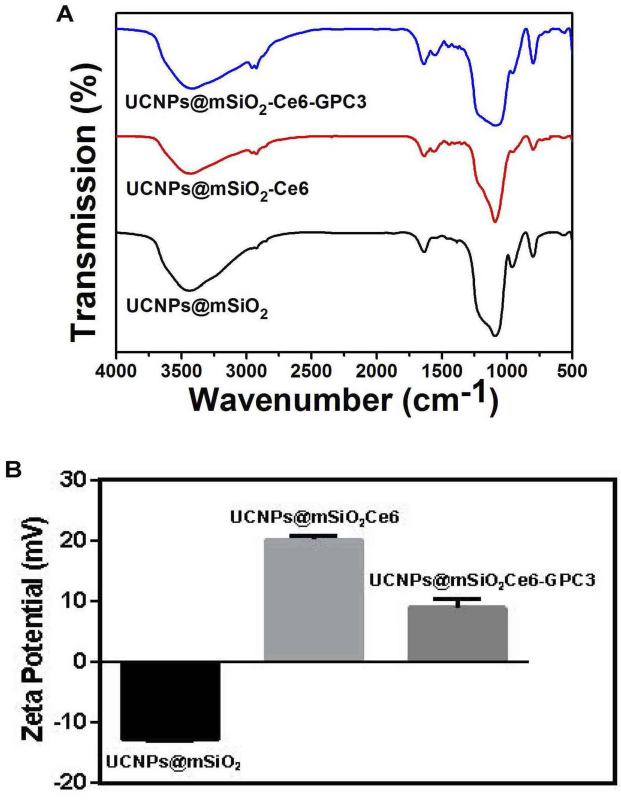

Figure 3 (**A**) FT-IR spectra of UCNPs@$mSiO_2$ (black line), UCNPs@$mSiO_2$-Ce6 (red line) and UCNPs@$mSiO_2$-Ce6-GPC3 (blue line). (**B**) Zeta potential of UCNPs@$mSiO_2$, UCNPs@$mSiO_2$-Ce6 and UCNPs@$mSiO_2$-Ce6-GPC3.

Cellular Uptake Of UCNPs@$mSiO_2$-Ce6-GPC3 By HepG2 Cells

HepG2 cells overexpress GPC3.[28] L02 is the normal liver cell line with GPC3-negative expression.[29] GPC3 is readily accessible for antibody-mediated targeting and binding.[30] Flow cytometry showed that the GPC3-expressing HepG2 cells were specifically targeted the GPC3-NPs, the GPC3-nanoparticles only localized to the cell surface of HepG2 cells under confocal microscopy.[30] In this study, the cells were incubated with 500 μg mL^{-1} UCNPs@$mSiO_2$-Ce6-GPC3 NPs for 0.5 hr, 1 hr, and 3 hrs. UCNPs@$mSiO_2$-Ce6-GPC3 performed green fluorescence (Figure 4). The blue fluorescence from DAPI was used to stain the nuclei, the overlay of the two channels was also presented. In L02 cells, there was almost no green stain. In the first 0.5 hr, only small green spots were viewed in HepG2 cells, it indicated that a few of the UCNPs@$mSiO_2$-Ce6-GPC3 had been uptaken. Almost all HepG2 cells swallowed UCNPs@$mSiO_2$-Ce6-GPC3 after co-cultivation for 3 hrs.

Biocompatibility Of Nanomaterials In Vitro

The colorimetric MTT assay has been proved to be a relevant predictor for biocompatibility performance, we utilized human normal liver cell line L02 cells to evaluate the biocompatibility of UCNPs@$mSiO_2$, UCNPs@$mSiO_2$-Ce6 and UCNPs@$mSiO_2$-Ce6-GPC3 at different concentrations (7.8 to 500 mg mL^{-1}). Figure 5A shows that when the dose of the samples was as high as 500 μg mL^{-1}, the cell viability was about 95%; it indicated that the samples had no obvious cytotoxicity to normal liver cells. We also performed a hemolysis test for different concentrations of UCNPs@$mSiO_2$-Ce6-GPC3 NPs (Figure 5B). The hemolytic capacity of UCNPs@$mSiO_2$-Ce6-GPC3 to normal human blood was still less than 0.05% even when the concentration of NPs was up to 500 μg mL^{-1}; the results proved the potential of UCNPs@$mSiO_2$-Ce6-GPC3 for intravenous administration. The MTT and hemolysis assay revealed that the UCNPs@$mSiO_2$-Ce6-GPC3 had good biocompatibility to normal human liver cells in vitro.

In Vitro Antitumor Properties

In order to test the in vitro therapeutic effect of the NPs excited by 808 nm laser, we co-cultured the human liver cancer HepG2 cells with different concentrations (7.8 to 500 mg mL^{-1}) of the UCNPs@$mSiO_2$, Ce6, UCNPs@$mSiO_2$-Ce6 or UCNPs@$mSiO_2$-Ce6-GPC3. The MTT in vitro cell proliferation assay was used for testing

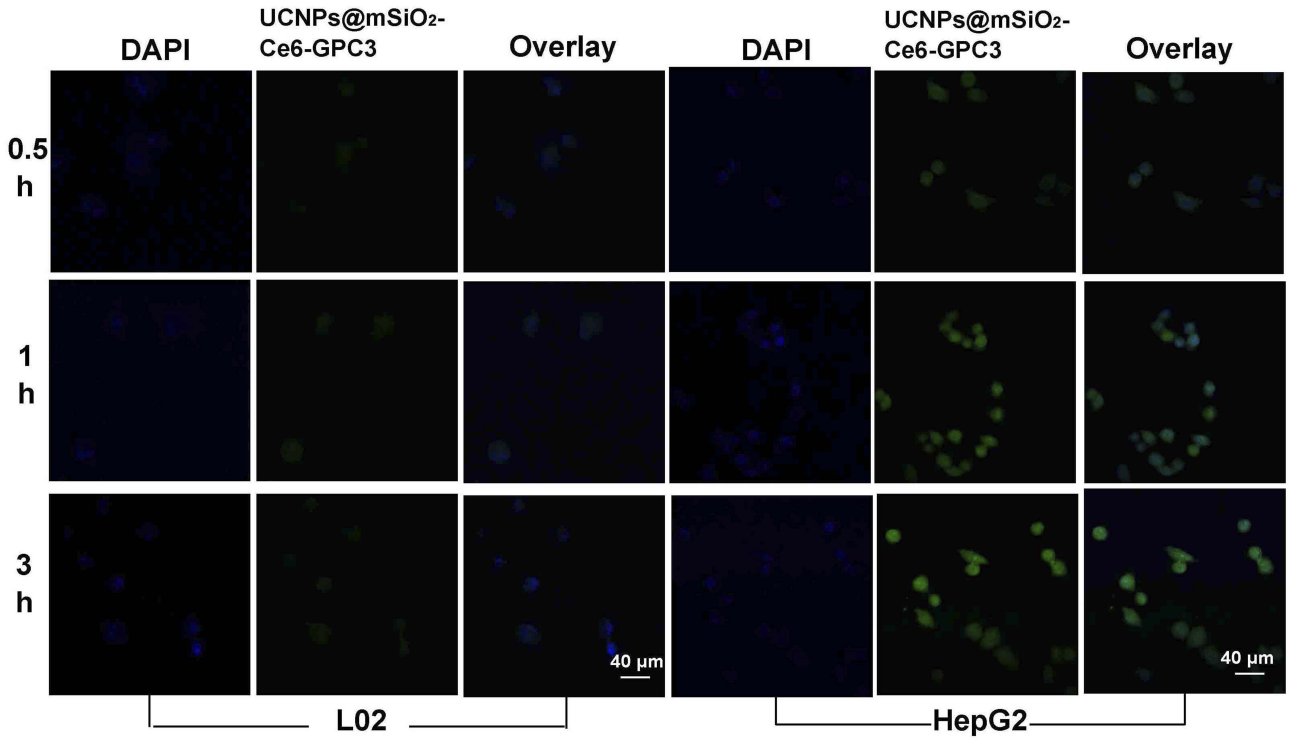

Figure 4 Confocal images of normal liver L02 cells and liver cancer HepG2 cells after co-incubation with DAPI and UCNPs@$mSiO_2$-Ce6-GPC3. The incubation time was 0.5 h, 1 h, 3 h; The left was the DAPI staining; The middle was the UCNPs@$mSiO_2$-Ce6-GPC3 image; The right was the overlay image of co-incubation with DAPI and the UCNPs@$mSiO_2$-Ce6-GPC3, scale bar 40 μm.

anticancer activity in our study. The groups of the materials were as follows: control (RPMI1640 medium), 808 nm NIR, UCNPs@$mSiO_2$+808 nm NIR, Ce6+808 nm NIR, UCNPs@$mSiO_2$-Ce6+808 nm NIR and UCNPs@$mSiO_2$-Ce6-GPC3+808 nm NIR. In Figure 6, the cell viability in 808 nm NIR groups and UCNPs@$mSiO_2$+808 nm NIR groups remained above 90%; it was suggested that the single 808 nm NIR had no obvious toxicity to the HepG2 cells, and the UCNPs@$mSiO_2$ vectors also did not have significant toxicity. Different concentrations of Ce6, UCNPs@$mSiO_2$-Ce6 or UCNPs@$mSiO_2$-Ce6-GPC3 were added to the HepG2 cells, 808 nm NIR irradiation with a pump power of 2 W cm^{-2} for 148 s was carried out. We found in UCNPs@$mSiO_2$-Ce6-GPC3+808 nm NIR groups, the HepG2 cells were more markedly killed in a NPs concentration-dependent manner (*P<0.05, **P<0.01); the cell viability was reduced to about 34% when the concentration of UCNPs@$mSiO_2$-Ce6-GPC3 was 500 μg mL^{-1}.

In Vivo Tumor Therapeutic Effects

We chose HepG2 subcutaneous xenograft model in nude mice to evaluate the anticancer efficacy of UCNPs@$mSiO_2$-Ce6-GPC3 under 808 nm laser irradiation in vivo. When the tumor long diameter was 6–8 mm, the mice were divided into 5 groups randomly, including control group, 808 nm NIR group, Ce6+808 nm NIR group, UCNPs@$mSiO_2$-Ce6+808 nm NIR group, UCNPs@$mSiO_2$-Ce6-GPC3+808 nm NIR group. For each treatment group, 0.1 mL of normal saline, Ce6, UCNPs@$mSiO_2$-Ce6 or UCNPs@$mSiO_2$-Ce6-GPC3 were injected to the tail vein. When the mice were treated with NIR, the tumor site was irradiated for 148 s at 2 W cm^{-2} with an 808 nm NIR laser. The mice were treated once every 7 days (the 0 day and the 6th day, the mice were sacrificed on the 14th day). With the prolonged time, the body weight of nude mice in all groups did not decrease, indicating the little side effect of UCNPs@$mSiO_2$-Ce6-GPC3 (Figure 7A). In Figure 7B, the tumor growth inhibition efficacy in Ce6+808 nm NIR, UCNPs@$mSiO_2$-Ce6+808 nm NIR and UCNPs@$mSiO_2$-Ce6-GPC3+808 nm NIR group was better than the control and single 808 nm NIR group. The mice in UCNPs@$mSiO_2$-Ce6-GPC3+808 nm NIR group had the lowest tumor volume (Figure 7B, *P<0.05 compared to control groups, n=5, Figure 7C and D). Researchers showed that laser stimulated skin and melanoma tumor growth. In our research, compared with the other groups, there were the largest tumor size in the single 808 nm NIR group (Figure 7B–D).

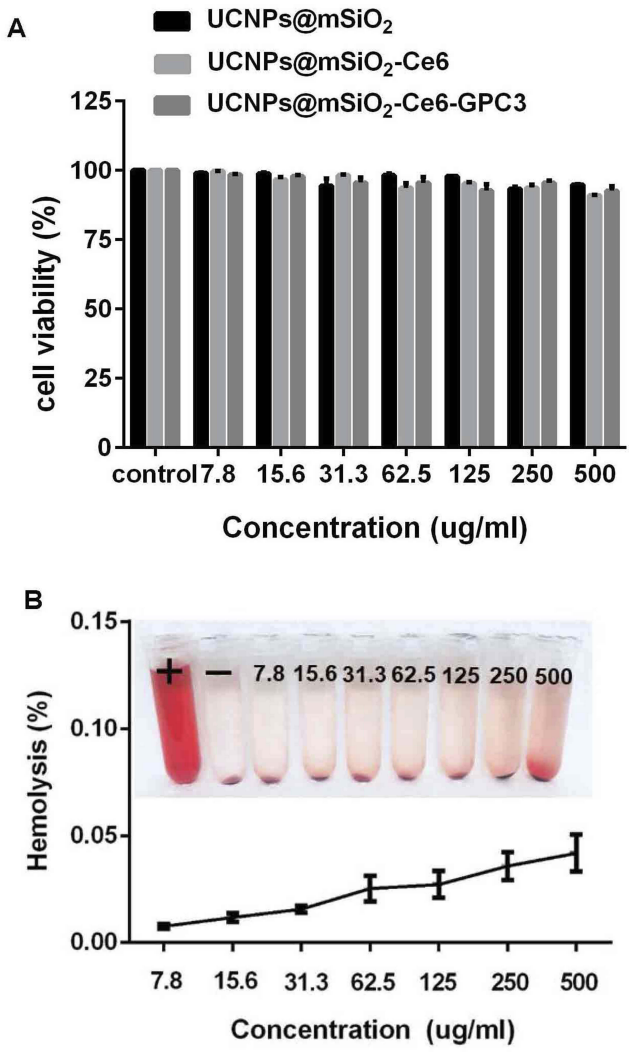

Figure 5 (**A**) The MTT assay using L02 cell lines incubated with different concentrations of UCNPs@mSiO$_2$, UCNPs@mSiO$_2$-Ce6 and UCNPs@mSiO$_2$-Ce6-GPC3. (**B**) The hemolysis assay of UCNPs@mSiO$_2$-Ce6-GPC3 using human blood red cells.

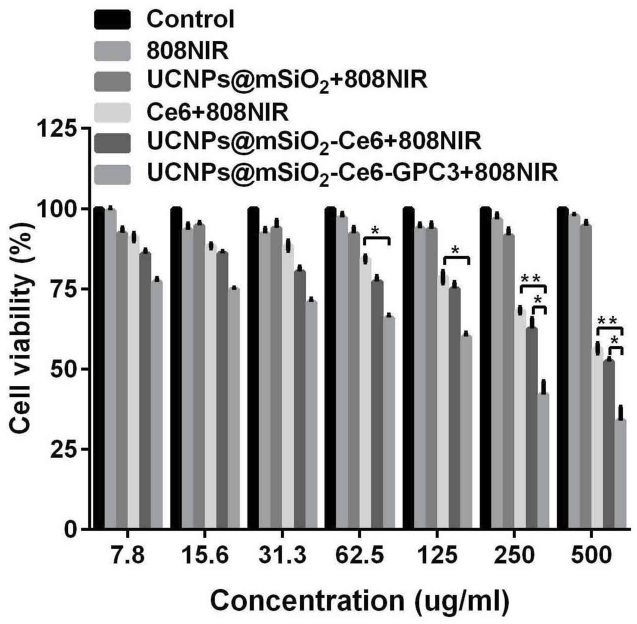

Figure 6 In vitro cell viability of HepG2 cells after treating with RPMI1640 medium (control group), 808 nm NIR, varied concentrations of UCNPs@mSiO$_2$, Ce6, UCNPs@mSiO$_2$-Ce6 and UCNPs@mSiO$_2$-Ce6-GPC3 plus 808 nm NIR (*P<0.05, **P<0.01).

Histology Examination

Hematoxylin and eosin-stained images of the tumor, heart, lung, liver, spleen and kidney in different groups after 14 days treatment were presented in Figure 8. Histology analysis of these organs from mice after injection of UCNPs@mSiO$_2$-Ce6-GPC3 with 808 nm NIR laser irradiation showed that the increased apoptotic and necrotic liver cancer cells could be found in the tumor. But there was no appreciable damage to the organs of heart, lung, liver, spleen or kidney.

Discussion

We used Nd^{3+} as a UCNP sensitizer that can be stimulated by 808 nm NIR. The core-shell-shell NPs are shown in Figure 1A. Energy could be smoothly transferred from Nd^{3+} to Yb^{3+} and then transferred to the activator. The inert layer could effectively prevent the energy from being transferred from the activator to back Nd^{3+} so that with this structure we could obtain high-intensity upconversion emission. Therefore, the upconversion luminescence of the UCNPs under 808 nm NIR illumination could be used to stimulate the photosensitizer to produce singlet oxygen to kill tumor cells.

The silica used for these nanocomposites had a suitable mesoporous size, a relatively large specific surface area, good biocompatibility and an easily modified surface. These properties make mesoporous silica a good carrier for a range of drugs to be supported by nanomaterials.[31] The TEOS underwent a series of hydrolysis condensation reactions at pH>7 and became a SiO_2 layer-coated nanoparticle. We coated the UCNPs with a layer of mesoporous silica. GPC3 is overexpressed in most human hepatocellular cancers and it is accessible for antibody-mediated binding and targeting via attachment to the cell membrane.[30] GPC3 is promising for targeted PDT for liver cancer. The UCNPs coated with the silica shell were amino-functionalized. The carboxyl groups of Ce6 and the GPC3 antibody terminus were activated by the carbodiimide method. Ce6 and the GPC3 antibody were successfully loaded onto the surface of

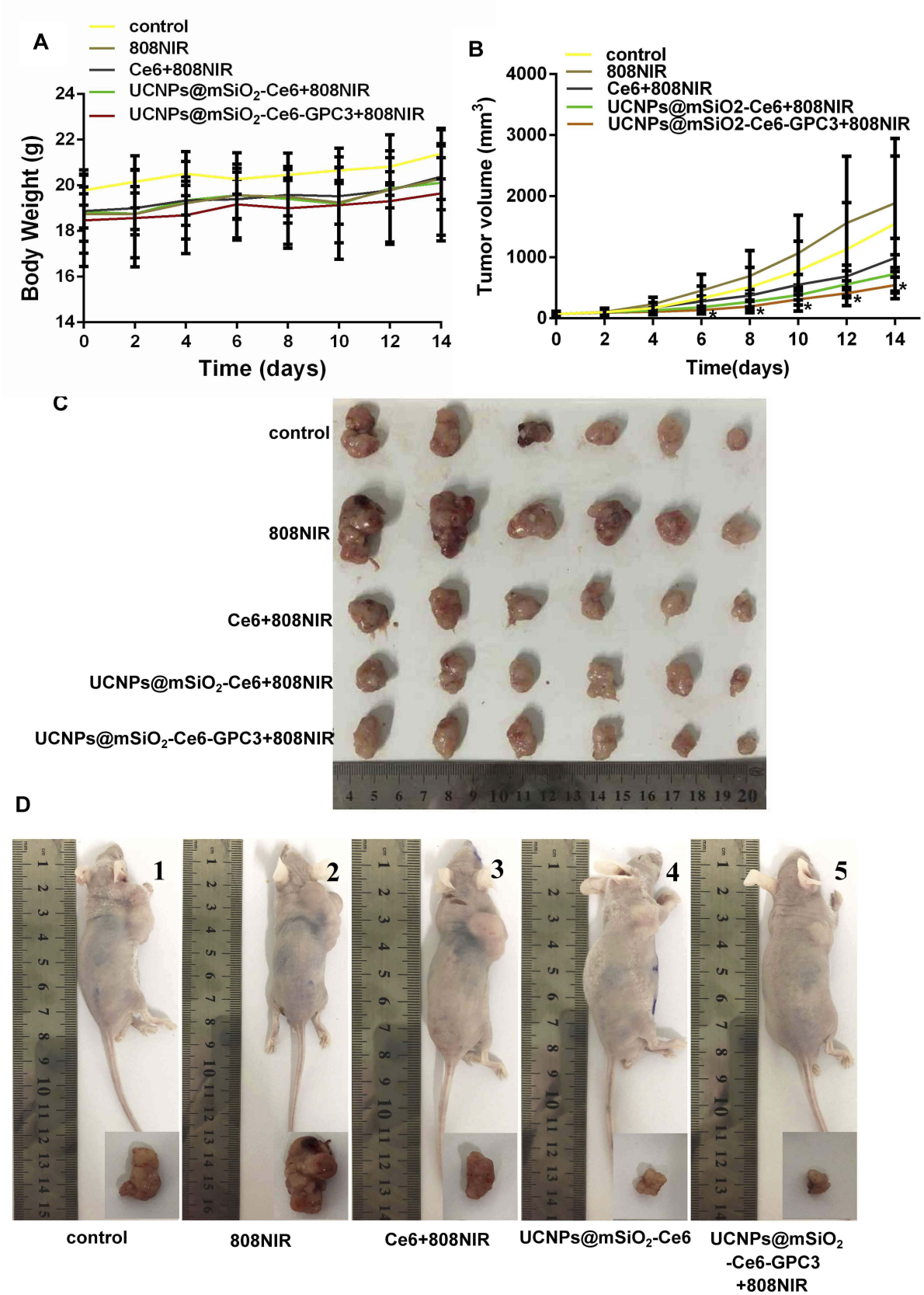

Figure 7 In vivo anti-cancer properties. (**A**) The body weight and (**B**) the tumor volume of nude mice in different groups versus the treatment time (*P<0.05 compared to control groups). (**C**) Tumor size in each treatment group. (**D**) Representative digital photographs of tumor-bearing mice and tumor tissue excised from tumor-bearing mice treated with (1) Control (normal saline), (2) 808 nm NIR, (3) Ce6+808 nm NIR, (4) UCNPs@mSiO$_2$-Ce6+808 nm NIR and (5) UCNPs@mSiO$_2$-Ce6-GPC3+808 nm NIR irradiation on the 14th day.

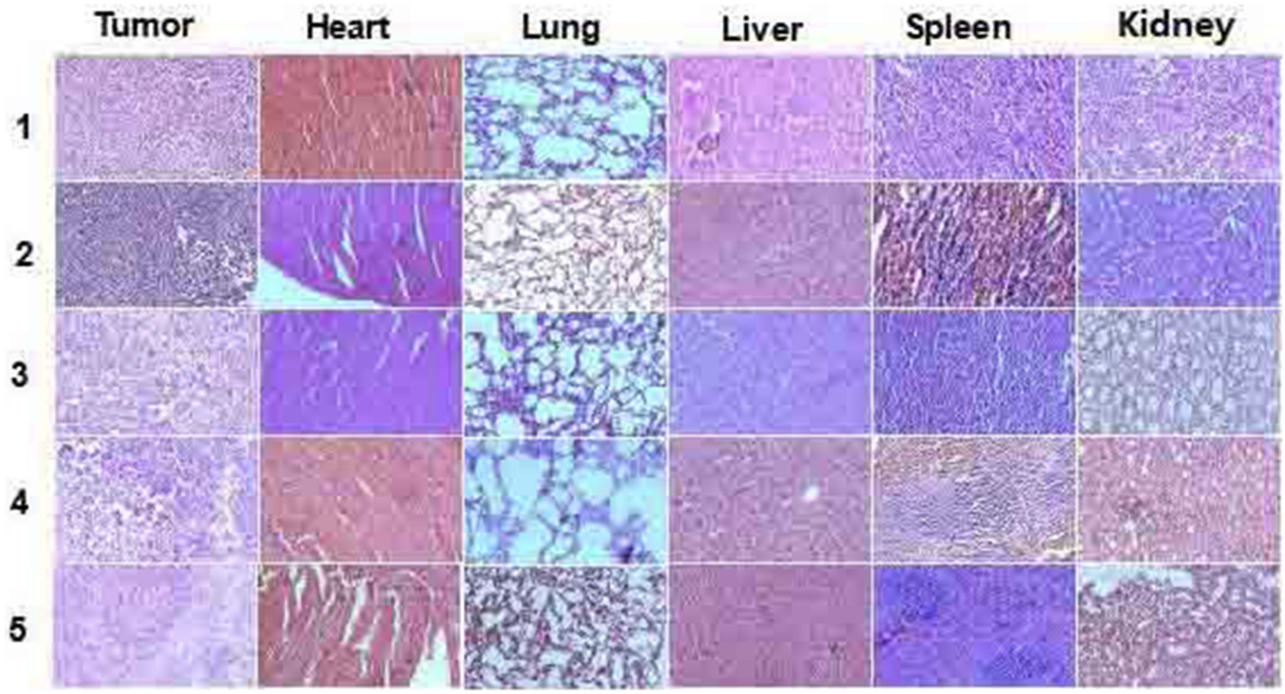

Figure 8 H&E-stained images of tumor, heart, lung, liver, spleen and kidney collected from different groups ((1) control (normal saline), (2) 808 nm NIR, (3) Ce6+808 nm NIR, (4) UCNPs@mSiO$_2$-Ce6+808 nm NIR and (5) UCNPs@mSiO$_2$-Ce6-GPC3+808 nm NIR) on the 14th day.

UCNPs@mSiO$_2$ to construct a system with targeted photodynamic effects.

We made the NPs and in every step, they had good dispersity and a very uniform size in cyclohexane, and the dispersity of UCNPs was maintained well after SiO$_2$ loading. The hexagonal phase and high crystallinity of the UCNPs were confirmed by powder X-ray diffraction and transmission electron microscopy. We optimized the luminescent properties of the materials. Three-layered NPs such as these have a relatively large diameter. Studies have shown that appropriately increasing the NP size will be extremely effective to increase the upconversion luminescence efficiency.[32]

To visually detect the phagocytic effect of UCNPs@mSiO$_2$-Ce6-GPC3 by HepG2 cells, we photographed the cells cocultured with 500 μg mL^{-1} UCNPs@mSiO$_2$-Ce6-GPC3 NPs for 0.5 hr, 1 hr, and 3 hrs with confocal microscopy. The ratio of the green signal in the cells and the coincidence of the green and the blue signals were enhanced with increasing time, and we obtained results showing that more particles were present in the cells.

A biocompatibility assay of the materials is necessary for a bioapplication research. It was shown that the viability of the Gd^{3+} complex-modified NaLuF4-based upconversion nanophosphors is approximately 80%.[33] In our study, the viability was 90–100% even when the entire dose range of the samples was as high as 500 μg mL^{-1}, which indicated that our materials had high biocompatibility. The hemolytic test with human red blood cells was applied to further confirm the biocompatibility in vitro, and we obtained negligible hemolysis results. These results were indicative of the good compatibility of UCNPs@mSiO$_2$-Ce6-GPC3.

We used the standard MTT assay to measure the anti-tumor therapeutic efficiency. The results of this assay indicated that the UCNPs@mSiO$_2$ vectors and pure 808 nm NIR have no cytotoxicity to HepG2 cells (Figure 6). When the cells were incubated with Ce6 or UCNPs@mSiO$_2$-Ce6 under 808 nm NIR laser irradiation, we obtained a much lower cell viability due to the PDT effect. The cells were treated with UCNPs@mSiO$_2$-Ce6-GPC3 and 808 nm NIR laser irradiation, and we found that the HepG2 cells were markedly restrained with a survival rate of approximately 34% The results showed that the photodynamic effect induced by 808 nm laser had obvious inhibition efficacy on hepatocellular carcinoma cells.

Body weight is a vital parameter to measure a material's systemic toxicity to the body. We found that the body weights of the mice in all treatment groups did not

decrease with prolonged treatment time, indicating small the little adverse side effects of UCNPs@mSiO$_2$-Ce6-GPC3 (Figure 7A). We previously reported that the UCNPs@MS-Au$_{25}$-PEG NPs possess efficient growth inhibition of tumors in vivo under 808 nm light irradiation.[34] Our study showed that the combination of UCNPs@mSiO$_2$-Ce6-GPC3 and 808 nm laser irradiation exhibited the best tumor growth inhibition in vivo (Figure 7B–D). It was interesting that the pure 808 nm laser irradiation (808 NIR group) showed the largest tumor size. Low-level laser therapy may either activate precancerous cells or increase the existing cancerous tissue.[35] Zhong et al reported that the skin turned black after treatment with a 980 nm laser.[36] Compared with the 980 nm laser, the 808 nm light showed less damaging effects to the skin. We did not detect a destructive effect from the 808 nm laser on the skin at the tumor site of the mice (Figure 7D).

Neither obvious apoptosis nor pathological changes were found in the heart, lung, liver, spleen, kidney or tumor cells, which indicated that our materials had no significant acute toxicity. However, the tumor cells were destroyed to various degrees with the combination of UCNPs@mSiO$_2$-Ce6-GPC3 and 808 nm NIR laser irradiation, and these results are in agreement with the tumor growth results. Thus, 808 nm NIR-excited UCNPs@mSiO$_2$-Ce6-GPC3 nanocomposites for PDT in liver cancer is a safe and feasible tumor treatment method.

Conclusion

In summary, the NaGdF4:Yb,Er@NaGdF4:Yb@NaNdF4:Yb(UCNPs) was prepared, we coated a layer of mesoporous silica on the surface and supported the photosensitizer Ce6 and anti-GPC3 through chemical bonding to successfully construct a dual treatment system for PDT and targeted therapy for liver cancer. The desired goal of simultaneous PDT and GPC3 targeted therapy were achieved at the cellular and animal levels. The platform had great potential and was highly expected to be used in the treatment of liver cancer.

Acknowledgments

This work was supported by National Natural Science Foundation of China (81401540), Innovation and Entrepreneurship Training Program for College Students in Heilongjiang Province (201710226080), Yu Weihan Academician's Outstanding Youth Training Fund in Harbin Medical University, Nn10 program (Nn10 PY 2017-03), Natural Science Foundation of Heilongjiang Province of China (LH2019H044), Youth Elite Training Fund (JY2015-02) and Outstanding Youth Fund (JCQN 2018-04) in Harbin Medical University Cancer Hospital. The abstract of this paper was presented at the 17th International Photodynamic Association World Congress as a poster presentation with interim findings.

Disclosure

The authors have no conflicts of interest to disclose.

References

1. Zeng H, Zheng R, Guo Y, et al. Cancer survival in China, 2003-2005: a population-based study. *Int J Cancer*. 2015;136(8):1921–1930. doi:10.1002/ijc.29227
2. Baskaran R, Lee J, Yang SG. Clinical development of photodynamic agents and therapeutic applications. *Biomater Res*. 2018;22:25. doi:10.1186/s40824-018-0140-z
3. Agostinis P, Berg K, Cengel KA, et al. Photodynamic therapy of cancer: an update. *CA Cancer J Clin*. 2011;61(4):250–281. doi:10.3322/caac.20114
4. Deng K, Li C, Huang S, et al. Recent progress in near infrared light triggered photodynamic therapy. *Small*. 2017;13(44). doi:10.1002/smll.201702299.
5. Kudinova NV, Berezov TT. Photodynamic therapy: search for ideal photosensitizer. *Biomed Khim*. 2009;55(5):558–569.
6. Huang L, Li Z, Zhao Y, et al. Ultralow-power near infrared lamp light operable targeted organic nanoparticle photodynamic therapy. *J Am Chem Soc*. 2016;138(44):14586–14591. doi:10.1021/jacs.6b05390
7. Abrahamse H, Hamblin MR. New photosensitizers for photodynamic therapy. *Biochem J*. 2016;473(4):347–364. doi:10.1042/BJ20150942
8. Kwiatkowski S, Knap B, Przystupski D, et al. Photodynamic therapy - mechanisms, photosensitizers and combinations. *Biomed Pharmacother*. 2018;106:1098–1107. doi:10.1016/j.biopha.2018.07.049
9. Zhou Z, Song J, Nie L, Chen X. Reactive oxygen species generating systems meeting challenges of photodynamic cancer therapy. *Chem Soc Rev*. 2016;45(23):6597–6626. doi:10.1039/c6cs00271d
10. Chen G, Qiu H, Prasad PN, Chen X. Upconversion nanoparticles: design, nanochemistry, and applications in theranostics. *Chem Rev*. 2014;114(10):5161–5214. doi:10.1021/cr400425h
11. Peng YP, Lu W, Ren P, et al. Multi-band up-converted lasing behavior in NaYF(4):Yb/Er nanocrystals. *Nanomaterials (Basel)*. 2018;8(7). doi:10.3390/nano8070497.
12. He F, Feng L, Yang P, et al. Enhanced up/down-conversion luminescence and heat: simultaneously achieving in one single core-shell structure for multimodal imaging guided therapy. *Biomaterials*. 2016;105:77–88. doi:10.1016/j.biomaterials.2016.07.031
13. Tian G, Zhang X, Gu Z, Zhao Y. Recent advances in upconversion nanoparticles-based multifunctional nanocomposites for combined cancer therapy. *Adv Mater*. 2015;27(47):7692–7712. doi:10.1002/adma.201503280
14. Wang Y, Wang H, Liu D, Song S, Wang X, Zhang H. Graphene oxide covalently grafted upconversion nanoparticles for combined NIR mediated imaging and photothermal/photodynamic cancer therapy. *Biomaterials*. 2013;34(31):7715–7724. doi:10.1016/j.biomaterials.2013.06.045
15. Li F, Du Y, Liu J, et al. Responsive assembly of upconversion nanoparticles for pH-activated and near-infrared-triggered photodynamic therapy of deep tumors. *Adv Mater*. 2018;30(35):e1802808. doi:10.1002/adma.201802808

16. Idris NM, Jayakumar MK, Bansal A, Zhang Y. Upconversion nanoparticles as versatile light nanotransducers for photoactivation applications. *Chem Soc Rev*. 2015;44(6):1449–1478. doi:10.1039/c4cs00158c
17. Kamkaew A, Chen F, Zhan Y, Majewski RL, Cai W. Scintillating nanoparticles as energy mediators for enhanced photodynamic therapy. *ACS Nano*. 2016;10(4):3918–3935. doi:10.1021/acsnano.6b01401
18. Chen X, Tang Y, Liu A, et al. NIR-to-red upconversion nanoparticles with minimized heating effect for synchronous multidrug resistance tumor imaging and therapy. *ACS Appl Mater Interfaces*. 2018;10(17):14378–14388. doi:10.1021/acsami.8b00409
19. Liu B, Chen Y, Li C, et al. Poly(Acrylic acid) modification of Nd3+-sensitized upconversion nanophosphors for highly efficient UCL imaging and pH-responsive drug delivery. *Advanced Functional Materials*. 2015;25(29):4717–4729. doi:10.1002/adfm.201501582
20. Liu Y, Kang N, Lv J, et al. Deep photoacoustic/luminescence/magnetic resonance multimodal imaging in living subjects using high-efficiency upconversion nanocomposites. *Adv Mater*. 2016;28(30):6411–6419. doi:10.1002/adma.201506460
21. Xie X, Gao N, Deng R, Sun Q, Xu QH, Liu X. Mechanistic investigation of photon upconversion in Nd(3+)-sensitized core-shell nanoparticles. *J Am Chem Soc*. 2013;135(34):12608–12611. doi:10.1021/ja4075002
22. Wu X, Yan P, Ren Z, et al. Ferric hydroxide-modified upconversion nanoparticles for 808 nm NIR-triggered synergetic tumor therapy with hypoxia modulation. *ACS Appl Mater Interfaces*. 2019;11(1):385–393. doi:10.1021/acsami.8b18427
23. Feng L, He F, Liu B, et al. g-C3N4Coated upconversion nanoparticles for 808 nm near-infrared light triggered phototherapy and multiple imaging. *Chem Mater*. 2016;28(21):7935–7946. doi:10.1021/acs.chemmater.6b03598
24. Xu M, Yang G, Bi H, et al. Combination of CuS and g-C3N4 QDs on upconversion nanoparticles for targeted photothermal and photodynamic cancer therapy. *Chemical Engineering Journal*. 2019;360(15):866–878. doi:10.1016/j.cej.2018.12.052
25. Baumhoer D, Tornillo L, Stadlmann S, Roncalli M, Diamantis EK, Terracciano LM. Glypican 3 expression in human nonneoplastic, preneoplastic, and neoplastic tissues: a tissue microarray analysis of 4,387 tissue samples. *Am J Clin Pathol*. 2008;129(6):899–906. doi:10.1309/HCQWPWD50XHD2DW6
26. Hanaoka H, Nagaya T, Sato K, et al. Glypican-3 targeted human heavy chain antibody as a drug carrier for hepatocellular carcinoma therapy. *Mol Pharm*. 2015;12(6):2151–2157. doi:10.1021/acs.molpharmaceut.5b00132
27. Tang X, Chen L, Li A, et al. Anti-GPC3 antibody-modified sorafenib-loaded nanoparticles significantly inhibited HepG2 hepatocellular carcinoma. *Drug Deliv*. 2018;25(1):1484–1494. doi:10.1080/10717544.2018.1477859
28. Wang Z, Han YJ, Huang S, et al. Imaging the expression of glypican-3 in hepatocellular carcinoma by PET. *Amino Acids*. 2018;50(2):309–320. doi:10.1007/s00726-017-2517-z
29. Dong L, Zhou H, Zhao M, et al. Phosphorothioate-modified AP613-1 specifically targets GPC3 when used for hepatocellular carcinoma cell imaging. *Mol Ther Nucleic Acids*. 2018;13:376–386. doi:10.1016/j.omtn.2018.09.013
30. Park JO, Stephen Z, Sun C, et al. Glypican-3 targeting of liver cancer cells using multifunctional nanoparticles. *Mol Imaging*. 2011;10(1):69–77.
31. Wang J, Han J, Zhu C, et al. Gold nanorods/polypyrrole/m-SiO2 core/shell hybrids as drug nanocarriers for efficient chemo-photothermal therapy. *Langmuir*. 2018;34(48):14661–14669. doi:10.1021/acs.langmuir.8b02667
32. Li J, Wu S, Zhang S. *Progress in Luminescence Efficiency of Up-Conversion Nanomaterials [EB/OL]*. Beijing: China Science and Technology Papers Online. Available from: http://www.paper.edu.cn/releasepaper/content/201207-135. Accessed July 12, 2012.
33. Xia A, Chen M, Gao Y, Wu D, Feng W, Li F. Gd3+ complex-modified NaLuF4-based upconversion nanophosphors for trimodality imaging of NIR-to-NIR upconversion luminescence, X-Ray computed tomography and magnetic resonance. *Biomaterials*. 2012;33(21):5394–5405. doi:10.1016/j.biomaterials.2012.04.025
34. He F, Yang G, Yang P, et al. A new single 808 nm NIR light-induced imaging-guided multifunctional cancer therapy platform. *Advanced Functional Materials*. 2015;25(25):3966–3976. doi:10.1002/adfm.201500464
35. Kara C, Selamet H, Gokmenoglu C, Kara N. Low level laser therapy induces increased viability and proliferation in isolated cancer cells. *Cell Prolif*. 2018;51(2):e12417. doi:10.1111/cpr.12417
36. Zhong Y, Tian G, Gu Z, et al. Elimination of photon quenching by a transition layer to fabricate a quenching-shield sandwich structure for 800 nm excited upconversion luminescence of Nd3+-sensitized nanoparticles. *Adv Mater*. 2014;26(18):2831–2837. doi:10.1002/adma.201304903

International Journal of Nanomedicine Dovepress

Publish your work in this journal

The International Journal of Nanomedicine is an international, peer-reviewed journal focusing on the application of nanotechnology in diagnostics, therapeutics, and drug delivery systems throughout the biomedical field. This journal is indexed on PubMed Central, MedLine, CAS, SciSearch®, Current Contents®/Clinical Medicine, Journal Citation Reports/Science Edition, EMBase, Scopus and the Elsevier Bibliographic databases. The manuscript management system is completely online and includes a very quick and fair peer-review system, which is all easy to use. Visit http://www.dovepress.com/testimonials.php to read real quotes from published authors.

Submit your manuscript here: https://www.dovepress.com/international-journal-of-nanomedicine-journal